Enhancement of Spot Weld Modeling using MAT_100_DAI

Falko Seeger[a], Markus Feucht[a], George Dumitru[b], Tobias Graf[b]
[a] Daimler AG, GR/VCS, HPC X603, 71059 Sindelfingen, Germany
{falko.seeger, markus.feucht}@daimler.com
[b] DYNAmore GmbH, Industriestraße 2, 70565 Stuttgart, Germany
{george.dumitru, tobias.graf}@dynamore.de

Summary:

During the recent years, the development of suitable and robust models for joining technologies has been advanced to augment the quality of full car crash simulations. Furthermore, the utilization of high-strength steel alloys and sophisticated joining concepts has led to an increased importance of joints in simulations.

On the basis of a fracture energy criterion, the bi-linear, elasto-plastic material model `MAT_SPOTWELD_DA` which already includes a stress based failure criterion will be enhanced to model the post failure behavior more precisely. Particularly, in complex structures with a series of joints at a flange, e.g. spot welds or rivets, the post failure behavior of the joints can control the overall behavior during crash. This new criterion has been implemented into LS-DYNA. In combination with the new possibilities in modeling single joints, the effects of the new options are validated and investigated on the basis of coupon as well as of component level.

Keywords:

Spot weld modeling, constitutive model and failure, crash worthiness, connection modeling,
finite element method, damage

1 Introduction

The modeling of the joint behavior at crash has gained a lot of importance during recent years. This development is caused by the demand to improve the quality of numerical models for crash simulation as well as the increased application of high and ultra-high strength steels. Especially in structures made by ultra-high strength steels, the joints are now a crucial point which can determine the behavior of the entire structure. A series of models were developed and investigated to reproduce the failure of joints, such as spot weld elements with force or stress based criteria [3, 5] or cohesive elements for modeling adhesive bonded structures [1, 2].

On the basis of existing failure models, a series of investigation were made to evaluate the capabilities at different levels of complexity. It can be concluded that beside the failure criterion, which covers the critical force, the post failure behavior plays an important role in the overall behavior. The potential of joints to resist a force along a certain displacement, and to dissipate energy, stabilizes structures in high speed loading cases and can ensure their integrity. For this reason, the post failure behavior has to be included into the material model.

2 Modeling of the Spot Weld

During the last year or even month, a lot of new features were implemented in LS-DYNA to cover the requirements of modeled spot welds and their failure behavior. Especially the discretization can now be done in several ways. Beside a simple solid element, the spot weld assembly (cluster) has to be established to model one spot weld with any number of solid elements [4]. The spot weld assembly provides advantages for the contact and internal forces, especially in the case of non-congruent meshes. Therefore, in this paper, a single spot weld will be modeled by a spot weld assembly containing eight linear hexahedron elements. Furthermore, the eight hexahedron cluster should be more robust regarding hourglass effects. Considering a single hexahedron element subjected to flexure will give the typical shape of an hourglass mode. The response and behavior of the hexahedron element is strongly influenced by the selected hourglass control.

2.1 Material model

For the description of the spot weld behavior of steel, `MAT_SPOTWELD_DA` was chosen to be appropriate among all the available material models. It is a simple bi-linear, elasto-plastic material model which behaves initially elastic until a defined yield stress σ_Y is reached. Later, a linear plastic behavior with E_{Tan} as hardening modulus is initiated, see Fig. 1(a). In `MAT_PLASTIC_KINEMATIC`, this model was enhanced to an elasto-viscoplastic material model by introducing the Cowper-Symond strain rate model.

Certainly, this simple material model allows only a rough approximation of the real behavior. But the real failure of the spot weld or any other joints is a complex mechanism and kinematic which has to be modeled with four or eight hexahedron elements. Therefore, it is not meaningful to apply a sophisticated material model using a coarse discretization for the spot weld. The methodology presented in this paper pursues a simple assumption.

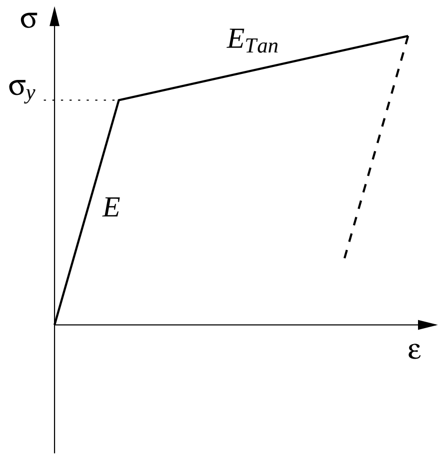

(a) Bi-linear, elasto-plastic material model

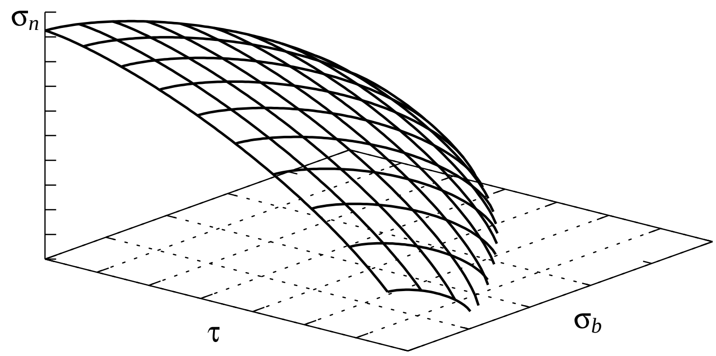

(b) Failure surface in the $(\sigma_n, \sigma_b, \tau)$-space

Figure 1: Material and failure model of MAT_SPOTWELD_DA

2.2 Failure criterion

The algorithm of the failure criterion implemented in MAT_SPOTWELD_DA determines internal stresses based on nodal forces via a simple beam theory. To cover the spot weld failure, a three dimensional stress-based failure criterion is used,

$$f = \left(\frac{\sigma_n}{S_n}\right)^{n_n} + \left(\frac{\sigma_b}{S_b}\right)^{n_b} + \left(\frac{\tau}{S_s}\right)^{n_s} \leq 1, \tag{1}$$

where S_n, S_b and S_s are the failure parameters for normal stress σ_n, bending stress σ_b and shear stress τ, respectively. The failure surface can take any arbitrary shape controlled by the three exponents n_n, n_b and n_s. To simplify the determination of the failure parameters, we assume

$$n = n_n = n_b = n_s. \tag{2}$$

Fig. 1(b) shows the failure surface – the failure parameters S_n, S_b and S_s are the intersections of the failure surface and the coordinate axis.

Including the failure parameters and the exponent, totally four free parameters have to be determined from the experiments. The KS2-specimen subjected to load angles of 0°, 30°, 60° and 90° as well as a coach peel test are the basis for the derivation of the failure parameters. In general, the exponent is defined by the KS2-experiments, whereas the coach peel test fixes the bending term.

3 Post Failure Behavior

In [5], a hyperbolic formulation is used to fade out the stresses of the spot weld element. It was mainly motivated by numerical aspects in order to prevent the release of mechanical energy in the same cycle when a spot weld element fails. Later investigations concerning spot weld modeling of body in white (BiW) crash simulation showed that the post failure behavior and the fracture energy mainly control the overall characteristics of the spot weld failure in those structures. The fracture energy determines the residual resistance of the spot weld. This phenomenon can be observed in adhesive bonded structures as well [2].

In this section, the material model will be enhanced by a so-called pseudo fracture energy, see Fig. 2. Compared to cohesive formulations, where at least two fracture modes are distinguished, only one fracture energy for tension as well as for shear is used, because its introduction is motivated by numerical aspects only. Generally, the material model can be divided now into 4 stages:

- elastic domain,
- plastic domain,
- failure criterion,
- damage or post failure behavior.

All sub-domains are passed through in sequential order without any interaction or relation in between. Theoretically, all sub-domains are replaceable with alternative models, e.g. the bi-linear, elasto-plastic material model could be substituted by `MAT_PIECEWISE_LINEAR_PLASTICITY`.

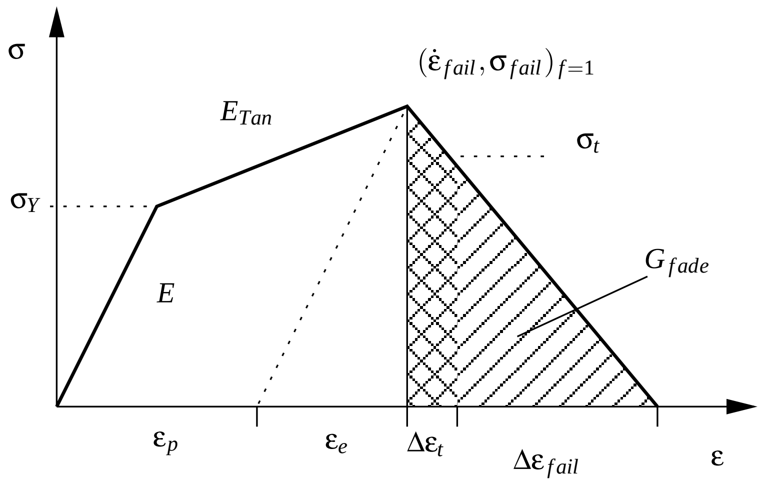

Figure 2: Introduction of fracture energy to control the fading of the stress

3.1 Scaled stress tensor

The approach concerning the damage behavior presented in this paper is based on a linear decrease of the internal stresses as a function of the strains, see Fig. 2. In general, there are several possibilities to implement such fading. One of the simplest ways is to calculate the number of remaining time steps using the effective strain rate at failure and scale down the stresses within this number of time steps – afterwards the element can be deleted. But this algorithm malfunctions already with changing strain rates.

Using `DG_TYP=3`, the damage d is calculated by the accumulated total strain increment $\Delta\varepsilon_{t+\Delta t}$, which is zero at failure, and the total fading strain increment $\Delta\varepsilon_{fade}$

$$d_{t+\Delta t} = \frac{\Delta\varepsilon_{t+\Delta t}}{\Delta\varepsilon_{fade}}, \tag{3}$$

with

$$\Delta\varepsilon_{t+\Delta t} \;=\; \Delta\varepsilon_t + \Delta t \sqrt{\frac{2}{3}\mathbf{D}_{t+\Delta t} : \mathbf{D}_{t+\Delta t}} \qquad \text{and} \qquad \Delta\varepsilon_{fade} \;=\; \frac{G_{fade}}{\sigma^v_{f=1}}\,. \tag{4}$$

Therein, $\Delta\varepsilon_{fade}$ is determined by the given fracture energy G_{fade} and the von Mises stress at failure $\sigma^v_{f=1}$, whereas $\mathbf{D}$ denominates the rate of deformation tensor. Afterwards the Cauchy stress tensor can be scaled using d by

$$\mathbf{T}_{t+\Delta t} \;=\; (1 - d_{t+\Delta t})\,\mathbf{T}_{f=1}. \tag{5}$$

The element will be deleted if $\Delta\varepsilon_{t+\Delta t}$ exceeds $\Delta\varepsilon_{fade}$.

In general, this algorithm provides the feature of fading out stresses over time. However, a few shortcomings can still be noticed. Since the algorithm is based on the von Mises stress, the correct behavior can only be obtained for a shearing load. In case of tension, the defined fracture energy is not computed correctly. For this reason, another method to calculate the damage d is considered.

In contrast to the prediction of the total fading strain in Eq. (4), the released rupture energy will be considered alternatively by

$$G_{t+\Delta t} \;=\; G_t + \Delta G_{t+\Delta t}, \tag{6}$$

with the rupture energy G at the times t and $t+\Delta t$ and its increment. The increment of the rupture energy or the current work can be expressed as follows:

$$\Delta G_{t+\Delta t} \;=\; \frac{1}{2}\Delta t\,(\mathbf{T}_{t+\Delta t} + \mathbf{T}_t) : \mathbf{D}_{t+\Delta t}. \tag{7}$$

Hence the stress tensor $\mathbf{T}_{t+\Delta t}$ of the current time step has to be calculated itself, the work increment will be approximated by

$$\Delta G_{t+\Delta t} \;\approx\; \Delta t\,\mathbf{T}_t : \mathbf{D}_{t+\Delta t}. \tag{8}$$

Similar to Eq. (5), the stress tensor at the point of failure $(f = 1)$ is scaled depending on the fracture energy:

$$\mathbf{T}_{t+\Delta t} \;=\; \left(1 - \frac{G^{ref}_{t+\Delta t}}{G_{fade}}\right)\mathbf{T}_{(f=1)}. \tag{9}$$

The unit of the fracture energy, which has to be defined in a LS-DYNA input deck later on, has a physical unit of $\mathrm{Nmm/mm^3}$. Therefore, the increment of the fracture energy has to be transformed into the reference configuration by

$$\Delta G^{ref}_{t+\Delta t} \;=\; \Delta t\,\det(\mathbf{F})\,\mathbf{T} : \mathbf{D}. \tag{10}$$

In general, the motivation to introduce a fracture energy for the definition of a fading out criterion is mainly driven by numerical aspects. The defined energy quantity in Eq. (10) might not probably fulfill all aspects of physical consistence, and therefore, it would be apt to identify it as pseudo fracture energy. This method ensures a monotonous decline of each stress component, whereas the fracture energy rises continuously. The main disadvantage of scaling stresses in Eq. (9) is switching-off any material behavior, which might cause instabilities. If two sequential combined load cases of pure tension and simple shear are considered, the solid element will distort non-physically. Since the stress tensor is fixed at $f = 1$ and only scaled by Eq. (9), the material behavior is switched off and no response of any deformation can be observed in the stress tensor. Consequently, this approach of the damage behavior has to be enhanced.

3.2 Updated material model

To ensure a correct behavior of the spot weld by any deformation, the material model has to be applied for every time step. The calculation of the damaged stress will be divided into three steps:

1. calculation of the stress tensor $\hat{\mathbf{T}}_{t+\Delta t}$,
2. calculation of the stress tensor $\mathbf{T}'_{t+\Delta t}$, which is equipotential to the stress tensor $\mathbf{T}_{(f=1)}$,
3. scaling of $\mathbf{T}'_{t+\Delta t}$ to determine $\mathbf{T}_{t+\Delta t}$.

The function of the algorithm is exemplary illustrated in Fig. 3 for a generic 2D stress state. σ has to be substituted by $\mathbf{T}$ for the further derivation.

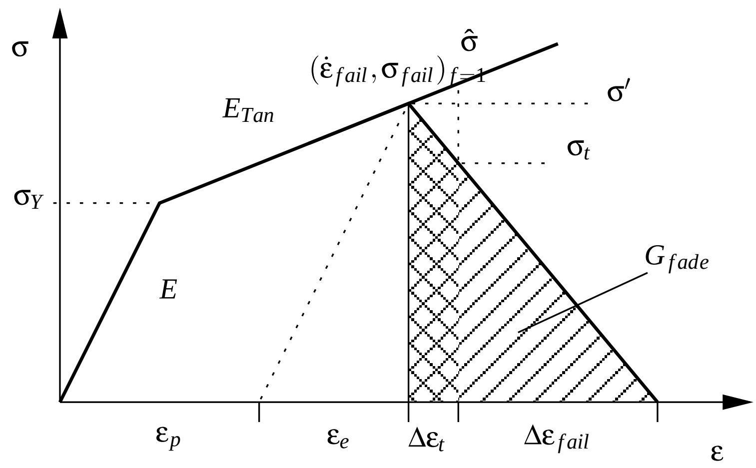

Figure 3: Enhancement of the damage algorithm to control the fading of the stress

By performing the first step, the stress tensor $\hat{\mathbf{T}}_{t+\Delta t}$ is calculated via the bi-linear, elasto-plastic material model. In general, it does not matter if the behavior of the solid element is elastic or plastic. For calculating $\mathbf{T}'_{t+\Delta t}$, it will be assumed that $\hat{\mathbf{T}}_{t+\Delta t}$ can be scaled with α:

$$\mathbf{T}'_{t+\Delta t} \quad = \quad \alpha \hat{\mathbf{T}}_{t+\Delta t}. \tag{11}$$

Multiplying this equation with the rate of deformation tensor $\mathbf{D}_{t+\Delta t}$, an energy based formulation can be obtained:

$$\mathbf{T}'_{t+\Delta t} : \mathbf{D}_{t+\Delta t} = \alpha \hat{\mathbf{T}}_{t+\Delta t} : \mathbf{D}_{t+\Delta t}. \tag{12}$$

With the second assumption of $\mathbf{T}'_{t+\Delta t} \approx \mathbf{T}'_t$, the scaling factor can be determined via

$$\alpha \approx \frac{\mathbf{T}'_t : \mathbf{D}_{t+\Delta t}}{\hat{\mathbf{T}}_{t+\Delta t} : \mathbf{D}_{t+\Delta t}}. \tag{13}$$

Finally, the damaged stress can be written by substituting Eq. (13) in Eq. (11) as

$$\mathbf{T}'_{t+\Delta t} = \frac{\mathbf{T}'_t : \mathbf{D}_{t+\Delta t}}{\hat{\mathbf{T}}_{t+\Delta t} : \mathbf{D}_{t+\Delta t}} \hat{\mathbf{T}}_{t+\Delta t}. \tag{14}$$

Considering Eq. (12), the stresses are scaled by an energy based criterion. This means that for a monotonic loading, the stress tensor $\mathbf{T}'$ will be constant as shown in Fig. 3. If the load changes, the constitution of the stress tensor will change as well as a response to the different deformation. Since the scalar product of $\mathbf{D}_{t+\Delta t}$ with $\mathbf{T}'_{t+\Delta t}$ contains the same energy increment in comparison to $\mathbf{T}'_t : \mathbf{D}_{t+\Delta t}$; the stress tensor $\mathbf{T}'_{t+\Delta t}$ is equipotential to the stress tensor $\mathbf{T}_{(f=1)}$.

Besides the energy based scaling of the undamaged stress tensor, it can be scaled alternatively by their norms with

$$\alpha^2 = \frac{\mathbf{T}'_t : \mathbf{T}'_t}{\hat{\mathbf{T}}_{t+\Delta t} : \hat{\mathbf{T}}_{t+\Delta t}}. \tag{15}$$

4 Single Element Test

Firstly, the behavior of the material model is studied on element level. A single eight-noded hexahedron element is subjected to a specific, well defined load case: pure tension and simple shear. Furthermore, a combined sequential load case, first a pure tension and afterwards a simple shear, is applied to the single element.

Fig. 4 shows the results for tension and shear load. It can be seen that the residual fracture energy decreases over time monotonic and linearly for the two cases, respectively. The more interesting case is shown in Fig. 5, where the load cases tension and shear are applied sequentially to the hexahedron element. The load case is switched from tension to shear at $t = 50$ as it can be clearly observed in Fig. 5(a). Similar to the single test, the residual fracture energy decreases linearly over time until the load is changed. Afterwards, the characteristic is non-linear because of the new stress state and the energy based formulation in Eq. (13). In general, the algorithm is able to cover a combined load case and to fade out the spot weld elements.

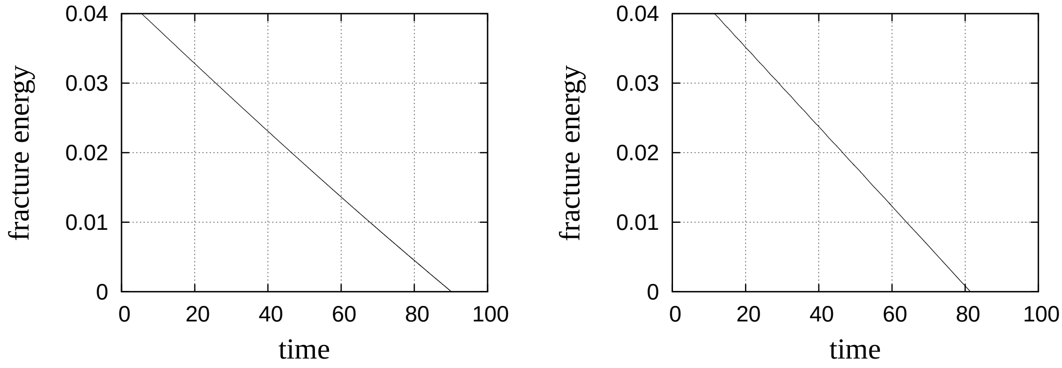

(a) Shear (b) Tension

Figure 4: Tension and shear load subjected to a single element

5 Coupon Level

Secondly, the fracture energy of the new damage model is determined on coupon level using KS2- and coach peel specimens. These specimens will be used to characterize the general behavior of a certain spot welded material/gage combination [3, 5]. This provides the basis to determine the material parameters as well as the failure parameters of the `MAT_SPOTWELD_DA`. The KS2-specimen can be subjected to loads of different angles of 0°, 30°, 60° and 90° to study the spot weld behavior under tension and shear as well as under combined shear-tension. The experiments are performed using controlled displacements with the resultant forces as output parameter.

The KS2-specimen including the test environment is modeled by shell elements with comparable properties and discretization of a BiW model, whereas a eight-hexahedron cluster represents the spot weld. The elasticity of the testing machine and the clamping device are taken into account by additional discrete beam elements which include their force-displacement characteristic. The force F is measured at a defined cross section, see Fig. 6.

The comparisons of experiments and simulation in Fig. 7 show a good correlation for the critical force. Concerning the displacement at failure, the model of the KS2-specimen behaves stiffer than it is in reality and a gap can be observed. Because of the coarse discretization of the flange with a element length of 5×5 mm, the bending state is poorly reproduced which led to these results. Regarding a BiW model, at

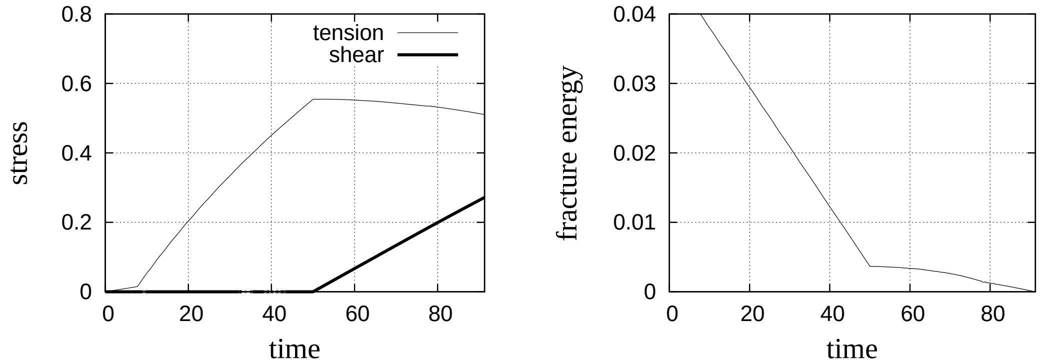

(a) Tesion and shear stresses (b) Fracture energy

Figure 5: Combined tension and shear load subjected to a single element in sequential order

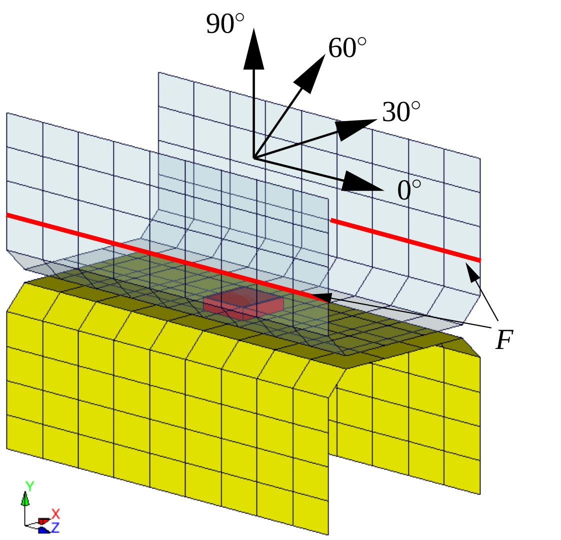

(a) Tensile-shear specimen (KS2)

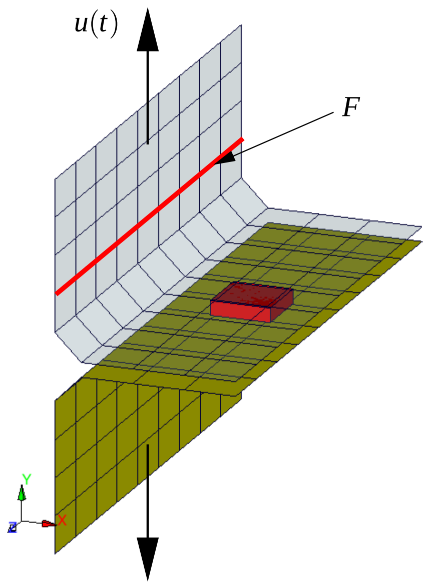

(b) Coach peel

Figure 6: Tested specimen on coupon level

first the spot weld failure model has to cover the critical forces. Furthermore, such large and localized deformations do not occur in a BiW model.

Nevertheless, a good post failure behavior with a defined damage can be observed. The setting of the

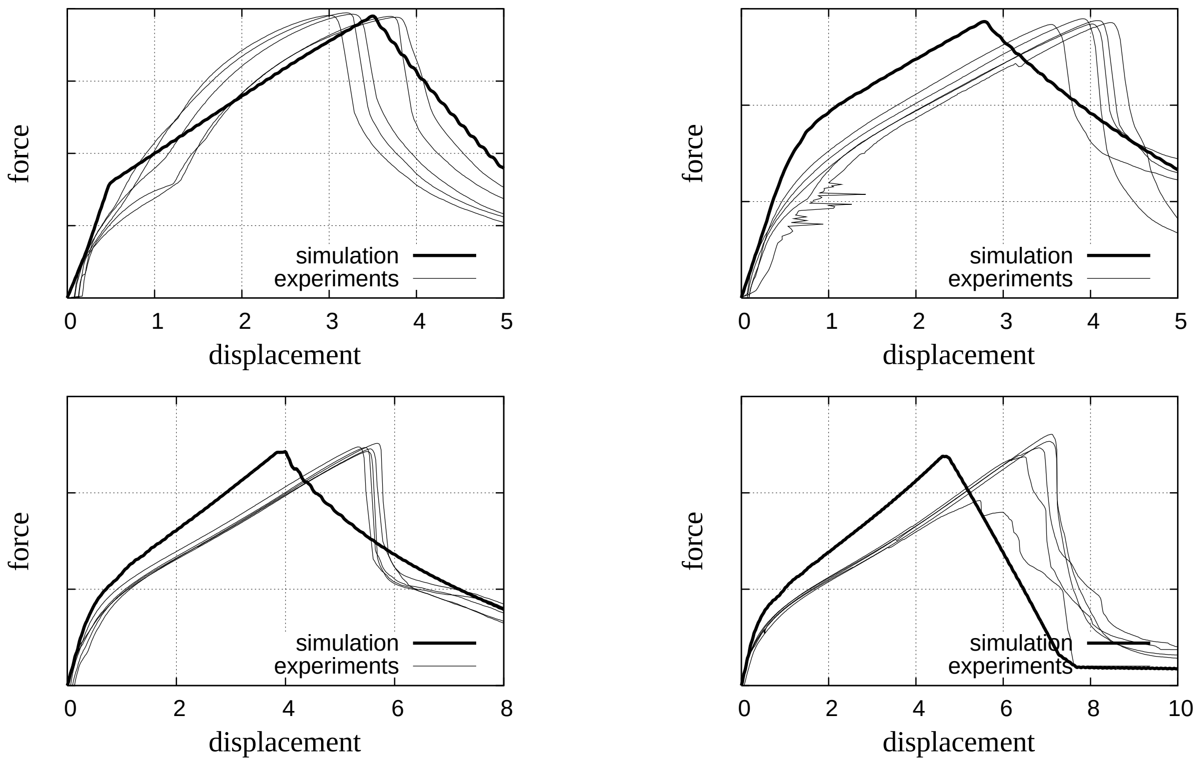

Figure 7: Comparison of experiments and simulation of a KS2-specimen for DP600; 1.5mm

fracture energy compromises all load cases since only one value of the energy is available. This parameter has to fit the shear as well as the tension load case.

6 T-Component

At last, the new damage model of MAT_SPOTWELD_DA is studied on the T-component test. The T-component consists of two main parts and is loaded by an impactor with $v = 2.5$ m/s, see Fig. 8. This test gives a possibility to study the interaction between several spot welds and their behavior under comparable realistic load conditions. The force is measured at the impactor by an integrated load cell, whereas the displacement is determined using an inductive displacement transducer. The characteristic is presented as a force-displacement-curve.

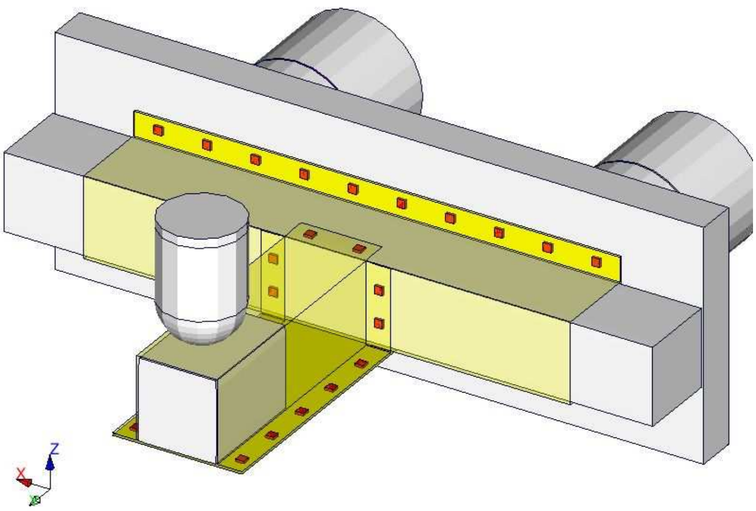

Figure 8: Model of the T-component

Fig. 9 shows the influence of the fracture energy. If no energy is defined, that means the post failure behavior is switched off, the force will decrease suddenly after the spotweld elements fail ($f = 1$). Using fracture energy, one has to distinguish between spot weld failure ($f = 1$) and deletion of the hexahedron elements. The spot welds will be damaged ($f = 1$) as well, but due to the fracture energy, they will not be deleted immediately. They are still able to carry a certain load and, therefore, the T-component does not fail at all.

7 Conclusion

Within this contribution, an enhancement of the material model MAT_SPOTWELD_DA was presented. Thereby, in contrast to the formulation used in DG_TYP=3, where the stress tensor of the spot weld is fixed at failure ($f = 1$) and scaled down, the constitutive relation between stresses and strains is further active during the post failure process. This means that the spot weld can still respond to load changes. The efficiency of the presented formulation was shown by several numerical examples, where a good agreement with KS2-experiments and a T-component test could be observed. Nevertheless, the presented model has to be validated at further KS-2 specimens and full car crash simulations.

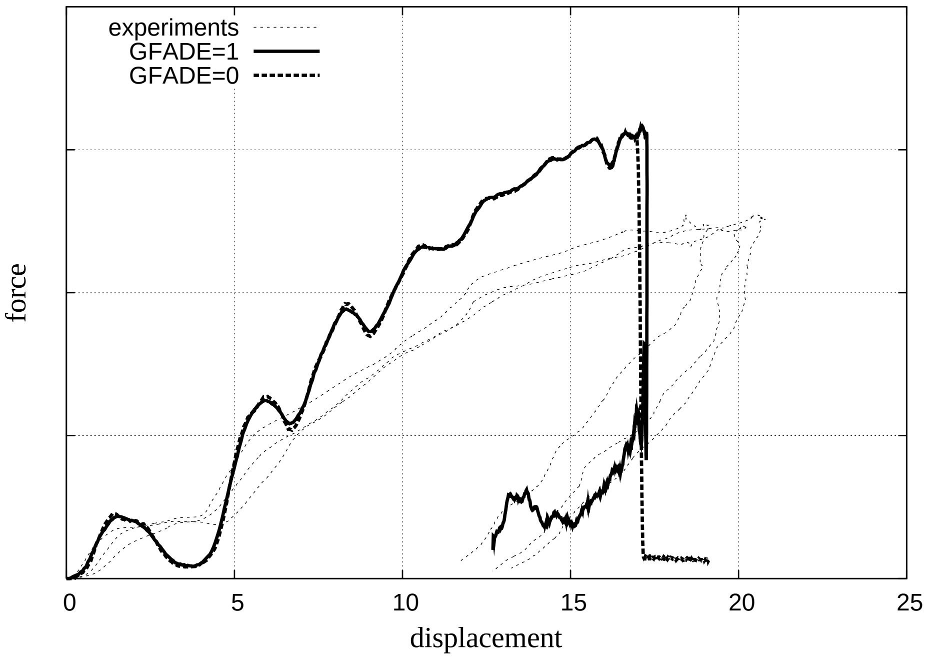

Figure 9: Influence of the fraction energy at the T-component

References

[1] *Abschlußbericht: Methodenentwicklung zur Berechnung von höherfesten Stahlklebverbindungen des Fahrzeugbaus unter Crashbelastung*, FOSTA P676, Oktober 2007

[2] Feucht, M., Haufe, A., Pietsch, G., *Modelling of Adhesive Bonding on Crash Simulation*, 6^{th} LS-Dyna Forum, Frankenthal 2007

[3] Hahn O., K. Özdem, M. Oeter, *Abschlußbericht: Experimentelle Bestimmung und rechnerische Vorhersage des Tragverhaltens punktgeschweißter Bauteile aus Stahlblechverbindungen unter Crashbelastung mit Hilfe von Ingenieurkonzepten*, FAT/ AVIF A172, Februar 2004

[4] Malcolm, S., Nutwell, E., *Spotweld Failure Prediction using Solid Element Assemblies*, 6^{th} European LS-Dyna Users' Conference, Gothenburg 2007

[5] Seeger, F., Feucht, M., Frank. Th., Keding, B., Haufe, A., *An Investigation on Spot Weld Modelling for Crash Simulation with LS-Dyna*, 4. LS-Dyna User Conference, Bamberg 2005